Measurement of pharmacokinetic parameters in histologically graded invasive breast tumours using dynamic contrast-enhanced MRI

RADJENOVIC, A., DALL, B. J., RIDGWAY, J. P. and SMITH, M. A.

Editorial Manager(tm) for The British Journal of Radiology
Manuscript Draft

Manuscript Number:

Title: Measurement of pharmacokinetic parameters in histologically graded invasive breast tumours using dynamic contrast enhanced MRI

Short Title: Pharmacokinetic analysis of graded breast tumours using DCE-MRI

Article Type: Full Paper

Section/Category: Physics & Technology

Keywords:

Corresponding Author: Dr Aleksandra Radjenovic,

Corresponding Author's Institution: University of Leeds

First Author: Aleksandra Radjenovic, MSc, PhD

Order of Authors: Aleksandra Radjenovic, MSc, PhD; Barbara J Dall, BSc, FRCR; John P Ridgway, MSc, PhD; Michael A Smith, PhD, FInstP

Manuscript Region of Origin:

Abstract: Dynamic contrast enhanced MRI (DCE-MRI) has demonstrated high sensitivity for detection of breast cancer. Analysis of correlation between quantitative DCE-MRI findings and prognostic factors (such as histological tumour grade) is important for defining the role of this technique in the diagnosis of breast cancer as well as the monitoring of neoadjuvant therapies.
This paper presents a practical clinical application of a quantitative pharmacokinetic model to study histologically confirmed and graded invasive human breast tumours. The hypothesis was that, given a documented difference in capillary permeability between benign and malignant breast tumours, a relationship between permeability-related DCE-MRI parameters and tumour aggressiveness persists within invasive breast carcinomas. In addition, it was hypothesised that pharmacokinetic parameters may

demonstrate stronger correlation with prognostic factors than the more conventional black-box techniques, so a comparison was undertaken.

Significant correlations were found between pharmacokinetic and black-box parameters in 59 invasive breast carcinomas. However, statistically significant variation with tumour grade was only demonstrated in two permeability related pharmacokinetic parameters: kep ($p<0.05$) and Ktrans ($p<0.05$), using one-way analysis of variance. Parameters kep, and Ktrans were significantly higher in Grade 3 tumours then in low grade tumours. None of the measured DCE-MRI parameters varied significantly between Grade 1 and Grade 2 tumours.

Measurement of kep and Ktrans might therefore be used to monitor the effectiveness of neoadjuvant treatment of high grade invasive breast carcinomas, but is unlikely to demonstrate remission in low grade tumours.

This piece of the submission is being sent via mail.

* Title Page

Measurement of pharmacokinetic parameters in histologically graded invasive breast tumours using dynamic contrast enhanced MRI

A. Radjenovic, MSc, PhD[1]

B.J. Dall, FRCR[2]

J.P. Ridgway, MSc, PhD[3]

M.A. Smith, PhD, FInstP[4]

[1] Academic Unit of Medical Physics, University of Leeds, Leeds, UK

Level 10, Worsley Building, Clarendon Way

University of Leeds

Leeds LS2 9JT, United Kingdom

tel : +44 0113 343 8319

[2] Department of Radiology, United Leeds Teaching Hospitals NHS Trust, Leeds, UK

[3] Department of Medical Physics, United Leeds Teaching Hospitals NHS Trust, Leeds, UK

[4] Sheffield Hallam University, Sheffield, UK

Short title: Pharmacokinetic parameters in graded invasive breast tumours using DCE-MRI

Measurement of pharmacokinetic parameters in histologically graded invasive breast tumours using dynamic contrast enhanced MRI

Abstract

Dynamic contrast enhanced MRI (DCE-MRI) has demonstrated high sensitivity for detection of breast cancer. Analysis of correlation between quantitative DCE-MRI findings and prognostic factors (such as histological tumour grade) is important for defining the role of this technique in the diagnosis of breast cancer as well as the monitoring of neoadjuvant therapies.

This paper presents a practical clinical application of a quantitative pharmacokinetic model to study histologically confirmed and graded invasive human breast tumours. The hypothesis was that, given a documented difference in capillary permeability between benign and malignant breast tumours, a relationship between permeability-related DCE-MRI parameters and tumour aggressiveness persists within invasive breast carcinomas. In addition, it was hypothesised that pharmacokinetic parameters may demonstrate stronger correlation with prognostic factors than the more conventional black-box techniques, so a comparison was undertaken.

Significant correlations were found between pharmacokinetic and black-box parameters in 59 invasive breast carcinomas. However, statistically significant variation with tumour grade was only demonstrated in two permeability related pharmacokinetic parameters: k_{ep} ($p<0.05$) and K^{trans} ($p<0.05$), using one-way analysis of variance. Parameters k_{ep}, and K^{trans} were significantly higher in Grade 3 tumours then in low grade tumours. None of the measured DCE-MRI parameters varied significantly between Grade 1 and Grade 2 tumours.

Measurement of k_{ep} and K^{trans} might therefore be used to monitor the effectiveness of neoadjuvant treatment of high grade invasive breast carcinomas, but is unlikely to demonstrate remission in low grade tumours.

Introduction

The blood circulation at the capillary level, or microcirculation, is determined by the metabolic activity of the tissue. In pathological processes (such as tumour genesis), the microcirculation becomes altered. There can be an increase in microvascular density resulting from the growth of new capillary networks (angiogenesis) as well as vasodilatation of existing vessels. With the relatively recent Federal Drug Administration's approval of drugs to target specifically angiogenesis, there is likely to be a requirement to monitor, non-invasively, the levels of angiogenic activity. Compartmental modelling using an MRI contrast agent gadopentetate dimeglumine (Gd-DTPA) and dynamic MRI acquisition offer the opportunity to investigate non-invasively and quantitatively the associated pharmacokinetics and hence the degree of angiogenic activity.

Gd-DTPA is an extracellular contrast agent which selectively alters the magnetic resonance signal intensity throughout its distribution volume which consists of plasma and extravascular extracellular fluid. Physiological parameters which determine tissue microcirculation have a direct influence on the resulting local bulk tissue concentration of Gd-DTPA following intravenous administration. It is therefore possible to monitor the patho-physiological status of tissues by measuring the temporal variation of the MR signal and qualitative information can be obtained from viewing the changes in image contrast. More importantly, it is also possible to obtain quantitative information associated with angiogenesis by mathematical analysis of dynamic contrast-enhanced MRI (DCE-MRI). The investigation of angiogenesis using DCE-MRI techniques can be divided into two fundamentally different groups: the so-called black-box methods and the more complex pharmacokinetic methods.

In black-box methods, the effect of Gd-DTPA is quantified in terms of heuristic, descriptive parameters describing the degree and the time course of enhancement [1-5]. These black-box parameters include maximal enhancement (ME), initial rate of enhancement (IRE), time to peak (TTP) and wash out slope (WOS). Arguably, this method of analysis does not utilise optimally the available data as information from only selected parts of the dynamic curves are used. Furthermore, it is not possible to correlate findings obtained by different pulse sequences or to compare parameters

measured in different centres. In quantifying the extent of Gd-DTPA induced contrast enhancement, no presumptions are made about the underlying physical or physiological processes. Although these parameters are certainly related to the physiological parameters that govern tissue microcirculation, the form of this relationship is not considered.

In contrast, the pharmacokinetic methods for quantitative analysis of DCE-MRI provide a framework that can be used to link the physics of MRI signal acquisition and the underlying patho-physiology that governs Gd-DTPA kinetics [6-9]. Pharmacokinetic (or compartmental) modelling of Gd-DTPA kinetics allows quantification of physiologically relevant parameters such as the volume of the extravascular extracellular space and capillary permeability. The development of methods for the quantification of DCE-MRI based on pharmacokinetic modelling has largely centred on cancer applications and the assessment of blood brain barrier integrity. Within the context of pharmacokinetic modelling it is theoretically possible to separate the influence of physical and physiological parameters on the measured changes of signal intensity in DCE-MRI, thus enabling an assessment of physiological parameters that characterise pathological microcirculation.

Since its introduction into clinical practice by Heywang-Kobruner in 1986 [10], DCE-MRI has almost unequivocally demonstrated high sensitivity for detection of breast cancer [11]. The main limitation of DCE-MRI in the investigation of breast lesions lies in its low specificity and the majority of studies in this field centred on the design of methods for improving the distinction between malignant and benign breast lesions. The most basic criterion for the differentiation between benign and malignant lesions is the presence or absence of enhancement; this, however, yields a specificity of only 37% [12]. Particularly problematic is the differentiation between benign fibroadenomas, ductal carcinoma in situ (DCIS), and some of the less angiogenesis-dependent types of cancer (such as invasive lobular carcinomas [13]). Improvement in DCE-MRI specificity in breast cancer (to 75-85%) can be achieved by its integration with other diagnostic findings and the formulation of precise inclusion criteria [13, 14].

The first reports of pharmacokinetic analysis of DCE-MRI were published in 1990 and 1991 by three independent European research groups in Copenhagen [7], Heidelberg [6] and London [9]. They applied this technique to the assessment of the breakdown of the blood-brain barrier in multiple sclerosis [7, 9] and brain tumours [6, 7]. The potential of this approach for the assessment of microcirculatory properties of the tissues in a variety of other pathological states was quickly recognised. All subsequent models reported in the literature presented variations of these three principal models without radically changing the underlying methodology. Pharmacokinetic analysis of DCE-MRI was applied to the assessment of breast cancer [15-17], cervical cancer [18], colorectal cancer [19] and heart disease [20-22].

Although the three principal approaches rely on a common set of assumptions, they differ in the way the final formulation of the model-predicted tissue response curve is represented as a function of physiological parameters, and in the way these parameters are labelled and interpreted[23]. The key differences in the practical implementation of these models are in the treatment of the temporal variation of the Gd-DTPA concentration in plasma, the choice of input function (mode of injection) and the measurement of native (pre-contrast) longitudinal relaxation time T1.

Although DCE-MRI was initially applied to the assessment of brain lesions, it has subsequently been used in the evaluation of a variety of tumours, with the research into Gd-DTPA pharmacokinetics in breast tumours being particularly prominent. Pharmacokinetic analysis was applied in several clinical studies of DCE-MRI in breast lesions where the primary aim of the quantitative analysis was the differentiation between benign and malignant tumours. Significantly higher permeability-related quantifiers of DCE-MRI were reported in invasive breast carcinomas than in benign lesions, although a variable degree of overlap between these groups of lesions was also noted in all published studies, regardless of the choice of the analysis method[24-30].

A comparison between black-box and pharmacokinetic analysis of DCE-MRI has been only sporadically reported the literature and the results of these comparisons are equivocal. Müller-Schimpfle et al [31], for example, found that the application of pharmacokinetic modelling did not

result in the improvement in the discrimination between benign and malignant breast lesions when compared to black-box assessment. Hulka [27] and Mussurakis [24], on the other hand, reported that their pharmacokinetic parameters allowed a more specific classification of breast cancer lesions than black-box measurements (such as ER, ME and wash-out slope WOS). Whilst Müller-Schimpfle used Brix's model for the extraction of pharmacokinetic parameters, Hulka applied Larsson's method; Mussurakis used both Brix and Tofts methods and found them to be equivalent. Temporal resolution of DCE-MRI in the Müller-Schimpfle study was low (one minute) whereas Hulka and Mussurakis used DCE-MRI sets acquired with a markedly higher temporal resolution of twelve and six seconds, respectively. The different conclusions reached in these studies regarding the comparative utility of pharmacokinetic and black-box methods are at least partly attributable to the differences in the DCE-MRI acquisition protocols.

Only a few studies have attempted to directly correlate DCE-MRI findings with prognostic factors such as tumour grade and nodal status in clinical studies of breast cancer [32-36]. None of these studies included pharmacokinetic analysis of DCE-MRI. Their results appear to be inconclusive and contradictory. Whilst Mussurakis [33] and Bone [35] found a significant correlation between DCE-MRI and prognostic factors, Fischer [34] and Stomper [32] found no correlation between them. Different acquisition and sampling protocols have been employed in each of these studies, as well as different methods for quantitative analysis of DCE-MRI. Furthermore, there was a considerable variation in the number of patients/lesions studied, their histological mix, the method used for grading as well as the choice of prognostic factors that DCE-MRI was compared with (tumour grade, nodal status, DNA S-phase percentage as well as various immunohistochemical prognostic indicators). The temporal resolution of DCE-MRI acquisitions used in these studies ranged from 12 seconds [33], to seven minutes [35] with tissue coverage ranging from four targeted sagittal slices [33] to 64 transverse slices encompassing both breasts [35].

This paper presents a practical clinical application of a quantitative pharmacokinetic model [37] to study histologically confirmed and graded invasive human breast carcinomas and to investigate the capacity of pharmacokinetic measurements of permeability to reflect histological tumour grade and

node status. The hypothesis was that given a documented difference in capillary permeability between benign and malignant breast tumours, a relationship between permeability-related DCE-MRI parameters and tumour aggressiveness persists within invasive breast carcinomas. In addition it was hypothesised that pharmacokinetic parameters may demonstrate a stronger correlation with prognostic factors than the more conventional black-box techniques so a comparison was undertaken.

Methods

Pharmacokinetic model

After intravenous injection, Gd-DTPA is rapidly distributed throughout the plasma volume and extravasated into the extracellular space. There is evidence that no metabolic trapping of Gd-DTPA occurs within the body and that it is completely eliminated in an unchanged form by renal excretion [37]. Being a highly hydrophilic molecule, Gd-DTPA is unable to cross-cellular membranes. In an open two-compartment model of Gd-DTPA kinetics, the extravasation of Gd-DTPA from the central (plasma) compartment is represented by a transfer constant K^{trans}. The back flux of Gd-DTPA from the extravascular extracellular compartment into the plasma compartment is represented by a transfer constant $k_{ep} = K^{trans}/v_e$, where v_e denotes the fractional volume of the extracellular extravascular (leakage) space. Fractional elimination rate k_{el} represents the clearance of Gd-DTPA from plasma. Pharmacokinetic parameters K^{trans} and k_{ep} therefore reflect the process of Gd-DTPA transfer across the capillary wall and are thus related to capillary permeability.

The pharmacokinetic modelling technique used in this paper combines the features of two earlier methods of Brix [6] and Tofts [8, 9]. This model [38] describes the temporal variation of contrast agent concentration in the tissue of interest $C_t(t)$, as a function of two pharmacokinetic parameters: v_e, and k_{ep} , as shown in equation 1.

$$C_t(t) = v_e \frac{D(a_1 + a_2)}{T}\left\{u\left(\exp(k_{el}^W \tau) - 1\right)\exp\left(-k_{el}^W t\right) - v\left(\exp\left(k_{ep}\tau\right) - 1\right)\exp\left(-k_{ep} t\right)\right\} \quad (1)$$

where:

v_e is the fractional volume of extravascular, extra cellular fluid (unit free fraction)

k_{ep} is the fractional transfer rate (expressed in min^{-1})

$$v = 1/(k_{ep} - k_{el}^{W})$$

$$u = (k_{ep} / k_{el}^{W})\, v$$

k_{el}^{W} is the fractional elimination rate of 0.058 min^{-1} quoted by Weinmann et al [37]

a_1 and a_2 were determined from published data [37] and have the following values: a_1 = 3.99 kg l^{-1}, a_2 = 4.78 kg l^{-1} [9]

D is the injected dose of Gd-DTPA per kg body weight (D = 0.1 mmol kg^{-1})

T is the effective duration of the infusion

$\tau = t$ for $t \leq T$ and $\tau = T$ for $t > T$

For a spoiled gradient echo acquisition sequence, with repetition time TR, flip angle α, the following approximation can be used at low concentrations $C_t(t)$ to represent temporal variation of normalised signal intensity following intravenous injection of Gd-DTPA:

$$SI(t)/SI_0 = 1 + a\, C_t(t) \qquad (2)$$

where:

SI (t) is the signal intensity at time t

SI_0 is the pre-injection signal intensity (i.e. t=0)

$a = [(\exp(- TR / T1))/(1 - \exp(- TR / T1))] TR \alpha$

Pre-contrast longitudinal relaxation time (T1) can be measured or an assumed fixed value can be used. In our method we used a published value of 876ms [39]

The pharmacokinetic parameter K^{trans} (the transfer constant) is obtained from the product of k_{ep} and v_e (i.e. $k_{ep} \times v_e$). The three conventional pharmacokinetic parameters now extracted and presented are v_e, k_{ep} and K^{trans}.

Clinical implementation of the model

There were a number of criteria for the imaging protocol: (i) complete bi-lateral coverage of both breasts was required as one of the principal clinical objectives was the detection of possible multifocality, (ii) DCE-MRI was required to yield images of diagnostic quality, suitable for qualitative assessment by radiologists, (iii) the duration of the DCE-MRI acquisition was required to be short in order to minimise problems related to gross patient motion and patient discomfort.

All imaging was performed on a 1.5 T MRI scanner (Gyroscan ACS NT, Philips Medical Systems, Best, The Netherlands). The MR signal detection was performed with a standard bilateral breast coil. The selection of the imaging volume was performed following the acquisition of survey scans in three orthogonal directions ensuring complete coverage of both breasts.

A 2D multislice, T1-weighted spoiled gradient echo sequence was used (TR/TE/φ = 213/4.6/90°, FOV = 300 x 300mm, 25 slices, 4mm slice thickness, 12 dynamic scans with temporal resolution of Delta T = 32.5 second acquisition intervals, 154 × 256 image matrix, reconstructed to 256 × 256 matrix). The acquisition protocol was based on that proposed by Kuhl et al [5] and the total imaging time was 390 seconds. The patients were positioned prone with both breasts inside the breast coil. The imaging was performed in the transverse plane, with the imaging volume encompassing both breasts in all three dimensions.

A standard dose of 0.1 mmol per kilogram body weight of gadopentetate dimeglumine Gd-DTPA (Magnevist®, Schering, Berlin, Germany) was used. The Gd-DTPA injection was followed by a 10 ml saline flush. The duration of the contrast administration was T_{inf} = (Delta T)/2 and effective duration of the infusion (T) which was used for the modelling was approximated by 2 × T_{inf}. This approximation was based on the data reported by Andersen et al and Fritz-Hansen et al [20, 40] for short peripheral injections. Therefore, effective injection duration T was 32.5 seconds.

Figure 1 represents a pair of pre- and post-contrast images and a resulting subtraction image of the transverse slice cutting through the centre of the lesion. In routine clinical practice, the lesion is evaluated by placing a region of interest (ROI) on a subtraction image and displaying a SI/time curve on a MR console. The subtraction method is effective in delineating the extent of the lesion. However, these images are less suitable for the analysis of the internal architecture of the lesion and its relationship to the surrounding parenchyma.

To improve the visualisation of the lesions, parametric maps of the black-box parameters ME, IRE and WOS were computed on a voxel-by-voxel basis and displayed superimposed on grey-scale anatomical images (Figure 2). These parameters were extracted from dynamic curve for each voxel in the 3D array using algorithms implemented in C programming language. A three-point moving window algorithm encompassing temporal segments of 65 seconds was used for measurement of maximal enhancement over baseline (ME) and initial rate of enhancement (IRE). Parameter WOS (wash-out slope) was computed on a voxel-by-voxel basis by measuring the slope of the least-squares straight line through the fixed five-point window encompassing the last 130 seconds of the dynamic curves. Three resulting colour coded images were interrogated simultaneously. No segmentation or motion correction was applied and a uniform colour-coding scheme was used in all studies. The computation of colour-coded parametric maps effectively condensed the information contained in the original DCE-MRI datasets. Following the visual inspection of parametric images, ROI selection was performed using an image processing package Analyze^{TM} (Biomedical Imaging Resource; Mayo Foundation, Rochester, MN).

The three pharmacokinetic parameters (K^{trans}, v_e, and k_{ep}) were calculated for each dynamic curve derived from a user-selected ROI. All processing was performed using a computer program for non-linear least squares fitting employing the Levenberg-Marquardt algorithm adapted from Press [41]. The program was written in C programming language and run on a standard PC. The processing was performed in a single batch operation as no user input was required.

Patients

MRI examination of the breasts was performed in patients with breast lesions where conventional triple assessment (X-ray mammography, ultrasound and clinical examination) did not provide conclusive diagnosis and where further information about the extent of a known lesion and/or possible multifocality was being sought. The study was approved by the regional ethics review board and a written informed consent was obtained from every patient. From the total of 255 consecutive patients who underwent the MRI examination, surgery was subsequently carried out in 66 cases. A full pathology report, including tumour grade and lymph node status, was available for 53 patients (60 lesions). Tumour grading was performed using the Nottingham Prognostic Index for primary breast cancer [42]. In one examination, quantitative analysis was not possible due to excessive patient motion.

Full DCE-MRI analysis was undertaken retrospectively in 59 lesions (in 52 patients). All patients were female with a median age of 55 (ranging from 32 to 80). The lesions were classified according to their histological grade into three groups. Twelve lesions were found to be Grade 1 tumours, twenty-nine were Grade 2 and eighteen were Grade 3 tumours. Thirty lesions had negative node status and twenty-nine were node positive. Forty-four lesions were classified as invasive ductal carcinomas not otherwise specified (NOS), eleven were invasive lobular carcinomas, two were invasive tubular carcinomas and two were invasive mucinous carcinomas. Thirty-four out of fifty-nine lesions had a significant in-situ (DCIS) component. Table 1 presents a summary of the pathology grading and lymph node status for the set of fifty-nine evaluated lesions.

Following the inspection of parametric maps, the most representative (usually central) cross section was identified by a trained radiologist and a single circular 16-voxel ROI was placed close to the lesion rim and away from the necrotic, central areas, if present (Figure 3). Figure 4 illustrates dynamic curves extracted from two different lesions and the superimposed least squares lines obtained after non-linear fitting of the experimental data to the pharmacokinetic model. The corresponding pharmacokinetic and black-box parameters are listed in Table 2.

Statistical analysis

SPSS statistical software package (Version 13.0, SPSS, Chicago, IL) was used for statistical analysis. All statistical tests were performed at $\alpha = 0.05$ confidence level.

Results

The technique worked robustly in this group of patients, adding only 5 minutes on to the investigation time. Of all the tumours and patients studied the technique was only unsuccessful on one occasion (due to excessive patient motion).

A summary of the black-box and pharmacokinetic parameters is presented in Tables 3 and 4 respectively. The mean values of measured parameters and their standard deviations are listed for each of the three subgroups. A pattern can be seen with a number of parameters (IRE, WOS, K^{trans}, k_{ep}) with the parameter value changing in a consistent manner when compared to tumour grade. However, when a comparison is made of the pharmacokinetic and black-box parameters for the three different tumour groups using one way analysis of variance, statistically significant variation with tumour grade was only detected in K^{trans} ($p<0.005$) and k_{ep} ($p<0.05$), though the parameter WOS approaches significance ($p=0.054$).

The summary of results of the post-hoc analysis of the differences between individual groups of measurements is presented in Table 5. A Least Significant Difference correction for multiple comparisons was used. Whilst there were no significant differences between Grade 1 and Grade 2

tumours, Grade 3 tumours were significantly different from Grade 1 and Grade 2 tumours, with respect to k_{ep} and K^{trans}.

The correlation of the DCE-MRI parameters with tumour grade and with each other is listed in Table 6. There are significant correlations between tumour grade and WOS, k_{ep} and K^{trans} ($p<0.01$) and IRE ($p<0.05$). K^{trans} exhibited the highest degree of correlation with tumour grade (Spearman's $\rho = 0.473$ $p < 0.0005$). The data for K^{trans} for each tumour group is plotted in Figure 5.

There was no significant association between DCE-MRI parameters and nodal status (Student's t-test, $p>0.05$). Furthermore, groups with and without a significant DCIS component also did not vary significantly (Student's t-test, $p>0.05$).

Discussion

In our study, the pharmacokinetic parameter K^{trans} demonstrated a stronger relationship with tumour grade than the conventional black-box parameters, suggesting greater sensitivity to differences in microcirculation between different tumour grades.

The measurements obtained in this study are in good agreement with v_e and K^{trans} values in invasive breast carcinomas reported by Tofts et al (K^{trans} of 0.1 – 1.2 min^{-1} and v_e of 0.3 –0.8) [16], and den Boer et al (K^{trans} of 1.05 ± 0.75 min^{-1} and v_e of 0.47 ± 0.20) [28]. Whereas Tofts did not measure $T1_0$, den Boer included a pre-contrast measurement of $T1_0$ in the pharmacokinetic analysis. Our measurements of K^{trans} are somewhat higher than those obtained by Ikeda [30] (0.52 ± 0.22 min^{-1}) and Hulka et al [26, 27] (0.45 ± 0.22 min^{-1}) possibly as a result of different $C_p(t)$ models. Both Ikeda and Hulka have modelled $C_p(t)$ as a three-exponential function. None of these studies, however, included measurements of v_e and K^{trans} in subgroups of invasive cancers, defined by histological

grade or nodal status. Furthermore, the proportion of high-grade tumours and tumours of different histological type will have influenced the mean values of K^{trans} and v_e measured in all these studies.

Prior to undertaking this study a comparable measurement of permeability in different histological grades of human breast cancer had not, to our knowledge, been reported in the literature. Our measurements are in broad agreement with permeability-related measurements in invasive breast carcinomas in humans reported elsewhere in studies involving an unspecified mix of histological grades and nodal involvement [16, 28]. However Furman-Haran *et al.* have recently demonstrated the capacity of high resolution DCE-MRI to detect the differences in perfusion-related pharmacokinetic parameters between low-grade and high-grade invasive breast carcinomas [43].

Whilst it is not possible to trace all possible sources of discrepancy between the results presented in this study and other clinical studies where the relationship between tumour grade and black-box quantifiers of DCE-MRI was investigated, one probable source of variability lies in the different acquisition sensitivity to underlying T1 changes. The most T1-sensitive acquisition sequence was used by Stomper et al [32, 36]. However, their studies included only a small number of subjects, and the imaging volume encompassed only five contiguous slices. Fischer et al [34] conducted a large study but employed a sub-optimal acquisition protocol, with respect to both temporal resolution (1.5 minutes) and T1 sensitivity. In two studies where simple enhancement ratios displayed significant association with tumour grade [33, 35] and nodal status [33], T1 sensitivity was somewhat higher than that achieved by our acquisition protocol . Their superior T1 sensitivity, however, was associated with the concomitant loss of spatial coverage [33] and temporal resolution [35]. The present study provided a compromise between the conflicting requirements for high temporal and spatial resolution, tissue coverage and T1 sensitivity, all of which are important for determining the utility of breast cancer DCE-MRI examinations.

Pharmacokinetic analysis of DCE-MRI was put forward as a tool for non-invasive monitoring of the effects of neoadjuvant chemotherapy in breast cancer and the reduction in K^{trans} was associated with positive response to therapy [44, 45]. However, the reports presented in the literature to date are

contradictory. Whereas Manton et al report that pharmacokinetic parameters had no prognostic value [46], Padhani et al found that the change in K^{trans} was an accurate predictor of response [47].

In the present study, all lesions were evaluated by MRI before surgical excision without the administration of pre-surgical (neoadjuvant) chemotherapy. Successful neoadjuvant chemotherapy could be viewed as an effective downgrading of the tumour (e.g. from Grade 3 to Grade 2, or from Grade 2 to Grade 1). Therefore, our measurements of DCE-MRI pharmacokinetic parameters in graded primary breast carcinomas may offer an insight into the mechanisms involved in the monitoring of the effects of neoadjuvant chemotherapy by pharmacokinetic analysis of DCE-MRI.

There was a high degree of correlation between black-box and pharmacokinetic factors (Table 6). However, pharmacokietic parameters K_{trans} and k_{ep} exhibited the highest degree of correlation with tumour grade.

Furthermore, our results indicate that permeability related pharmacokinetic parameters K^{trans} and k_{ep} vary significantly between Grade 3 and Grade 2 tumours, whereas there is no significant difference between Grade 2 and Grade 1 tumours (Table 2). This suggests that pharmacological downgrading of Grade 3 tumours can be detected by measuring the changes in K^{trans} and k_{ep}, and that further remission (from Grade 2 to Grade 1) will not result in significant change in K^{trans} and k_{ep}.

Acknowledgements

We would like to thank The Wellcome Trust for their financial support. We are grateful to D. D. and S.E.B. for their assistance with data collection.

References

1. Heywang SH, Wolf A, Pruss E, Hilbertz T, Eiermann W, Permanetter W. MR imaging of the breast with Gd-DTPA: use and limitations. Radiology 1989;171(1):95-103.

2. Kaiser WA, Zeitler E. MR Imaging of the breast - Fast imaging sequences with and without Gd-DTPA - Preliminary observations. Radiology 1989;170(3):681-6.

3. Gilles R, Guinebretiere JM, Lucidarme O, Cluzel P, Janaud G, Finet JF*, et al.* Nonpalpable breast tumors - Diagnosis with contrast-enhanced subtraction dynamic MR imaging. Radiology 1994;191(3):625-31.

4. Boetes C, Barentsz JO, Mus RD, van der Sluis RF, van Erning L, Hendriks J*, et al.* MR characterization of suspicious breast lesions with a gadolinium enhanced Turboflash subtraction technique. Radiology 1994;193(3):777-81.

5. Kuhl CK, Mielcareck P, Klaschik S, Leutner C, Wardelmann E, Gieseke J*, et al.* Dynamic breast MR imaging: Are signal intensity time course data useful for differential diagnosis of enhancing lesions? Radiology 1999;211(1):101-10.

6. Brix G, Semmler W, Port R, Schad LR, Layer G, Lorenz WJ. Pharmacokinetic parameters in CNS Gd-DTPA enhanced MR imaging. J. Comput. Assist. Tomogr. 1991;15(4):621-8.

7. Larsson HBW, Stubgaard M, Frederiksen JL, Jensen M, Henriksen O, Paulson OB. Quantitation of blood-brain-barrier defect by magnetic resonance imaging and Gadolinium-DTPA in patients with multiple sclerosis and brain tumors. Magn.Reson.Med. 1990;16(1):117-31.

8. Tofts PS. Modeling tracer kinetics in dynamic Gd-DTPA MR imaging. J. Magn. Reson. Imaging 1997;7(1):91-101.

9. Tofts PS, Kermode AG. Measurement of the blood-brain-barrier permeability and leakage space using dynamic MR imaging: 1. Fundamental concepts. Magn.Reson.Med. 1991;17(2):357-67.

10. Heywang SH, Hahn D, Schmidt H, Krischke I, Eiermann W, Bassermann R*, et al.* MR imaging of the breast using gadolinium-DTPA. J. Comput. Assist. Tomogr. 1986;10(2):199-204.

11. Kuhl CK, Schild HH. Dynamic image interpretation of MRI of the breast. J. Magn. Reson. Imaging 2000;12(6):965-74.

12. Harms SE, Flamig DP, Hesley KL, Meiches MD, Jensen RA, Evans WP*, et al.* MR imaging of the breast with rotating delivery of excitation off resonance - Clinical experience with pathological correlation. Radiology 1993;187(2):493-501.

13. Kuhl CK. MRI of breast tumors. Eur. Radiol. 2000;10(1):46-58.

14. HeywangKobrunner SH, Viehweg P, Heinig A, Kuchler C. Contrast-enhanced MRI of the breast: Accuracy, value, controversies, solutions. Eur. J. Radiol. 1997;24(2):94-108.

15. Hoffmann U, Brix G, Knopp MV, Hess T, Lorenz WJ. Pharmacokinetic mapping of the breast - a new method for dynamic MR mammography. Magn.Reson.Med. 1995;33(4):506-14.

16. Tofts PS, Berkowitz B, Schnall MD. Quantitative analysis of dynamic Gd-DTPA enhancement in breast tumors using a permeability model. Magn.Reson.Med. 1995;33(4):564-8.

17. Port RE, Knopp MV, Hoffmann U, Milker-Zabel S, Brix G. Multicompartment analysis of gadolinium chelate kinetics: Blood-tissue exchange in mammary tumors as monitored by dynamic MR imaging. J. Magn. Reson. Imaging 1999;10(3):233-41.

18. Hawighorst H, Knapstein PG, Weikel W, Knopp MV, Zuna I, Knof A*, et al.* Angiogenesis of uterine cervical carcinoma: characterization by pharmacokinetic magnetic resonance parameters and histological microvessel density with correlation to lymphatic involvement. Cancer Res. 1997;57(21):4777-86.

19. Müller-Schimpfle M, Brix G, Schlag P, Engenhart R, Frohmuller S, Hess T*, et al.* Recurrent rectal cancer - diagnosis with dynamic MR imaging. Radiology 1993;189(3):881-9.

20. Fritz Hansen T, Rostrup E, Larsson HBW, Sondergaard L, Ring P, Henriksen O. Measurement of the arterial concentration of Gd-DTPA using MRI: A step toward quantitative perfusion imaging. Magn.Reson.Med. 1996;36(2):225-31.

21. Larsson HBW, Stubgaard M, Sondergaard L, Henriksen O. In-vivo quantification of the unidirectional influx constant for Gd-DTPA diffusion across the myocardial capillaries with MR imaging. J. Magn. Reson. Imaging 1994;4(3):433-40.

22. Larsson HBW, Fritz-Hansen T, Rostrup E, Sondergaard L, Ring P, Henriksen O. Myocardial perfusion modeling using MRI. Magn.Reson.Med. 1996;35(5):716-26.

23. Tofts PS, Brix G, Buckley DL, Evelhoch JL, Henderson E, Knopp M*, et al.* Estimating kinetic parameters from dynamic contrast-enhanced T1-weighted MRI of a diffusable tracer: Standardized quantities and symbols. J. Magn. Reson. Imaging 1999;10(3):223-32.

24. Mussurakis S, Buckley DL, Drew PJ, Fox JN, Carleton PJ, Turnbull LW*, et al.* Dynamic MR imaging of the breast combined with analysis of contrast agent kinetics in the differentiation of primary breast tumours. Clin. Radiol. 1997;52(7):516-26.

25. Knopp MV, Weiss E, Sinn HP, Mattern J, Junkermann H, Radeleff J*, et al.* Pathophysiologic basis of contrast enhancement in breast tumors. J. Magn. Reson. Imaging 1999;10(3):260-6.

26. Hulka CA, Edmister WB, Smith BL, Tan LJ, Sgroi DC, Campbell T*, et al.* Dynamic echo-planar imaging of the breast: Experience in diagnosing breast carcinoma and correlation with tumor angiogenesis. Radiology 1997;205(3):837-42.

27. Hulka CA, Smith BL, Sgroi DC, Tan LJ, Edmister WB, Semple JP*, et al.* Benign and malignant breast lesions - differentiation with echo-planar MR imaging. Radiology 1995;197(1):33-8.

28. den Boer JA, Hoenderop RK, Smink J, Dornseiffen G, Koch PW, Mulder JH*, et al.* Pharmacokinetic analysis of Gd-DTPA enhancement in dynamic three-dimensional MRI of breast lesions. J. Magn. Reson. Imaging 1997;7(4):702-15.

29. Daniel BL, Yen YF, Glover GH, Ikeda DM, Birdwell RL, SawyerGlover AM*, et al.* Breast disease: Dynamic spiral MR imaging. Radiology 1998;209(2):499-509.

30. Ikeda O, Yamashita Y, Takahashi M. Gd-enhanced dynamic magnetic resonance imaging of breast masses. Top. Magn. Reson. Imaging 1999;10(2):143-51.

31. Müller-Schimpfle M, Ohmenhauser K, Sand J, Stoll P, Claussen CD. Dynamic 3D-MR mammography: Is there a benefit of sophisticated evaluation for enhancement curves for clinical routine? J. Magn. Reson. Imaging 1997;7(1):236-40.

32. Stomper PC, Penetrante RB, Edge SB, Arredondo MA, Blumenson LE, Stewart CC. Cellular proliferative activity of mammographic normal dense and fatty tissue determined by DNA S phase percentage. Breast Cancer Res. Treat. 1996;37(3):229-36.

33. Mussurakis S, Buckley DL, Horsman A. Dynamic MR imaging of invasive breast cancer: Correlation with tumour grade and other histological factors. Br. J. Radiol. 1997;70(833):446-51.

34. Fischer U, Kopka L, Brinck U, Korabiowska M, Schauer A, Grabbe E. Prognostic value of contrast-enhanced MR mammography in patients with breast cancer. Eur. Radiol. 1997;7(7):1002-5.

35. Bone B, Aspelin P, Bronge L, Veress B. Contrast-enhanced MR imaging as a prognostic indicator of breast cancer. Acta Radiol. 1998;39(3):279-84.

36. Stomper PC, Herman S, Klippenstein DL, Winston JS, Edge SB, Arredondo MA*, et al.* Suspect breast lesions - Findings at dynamic gadolinium enhanced MR imaging correlated with mammographic and pathological features. Radiology 1995;197(2):387-95.

37. Weinmann HJ, Laniado M, Mutzel W. Pharmacokinetics of Gd-DTPA dimeglumine after intravenous-injection into healthy volunteers. Physiol. Chem. Phys. Med. NMR 1984;16(2):167-72.

38. Radjenovic A, Ridgway JP, Smith MA. A method for pharmacokinetic modelling of dynamic contrast enhanced MRI studies of rapidly enhancing lesions acquired in a clinical setting. Phys. Med. Biol. 2006;51:N187–N97.

39. Merchant TE, Thelissen GRP, Degraaf PW, Nieuwenhuizen C, Kievit HCE, Denotter W. Application of a mixed imaging sequence for MR imaging characterization of human breast disease. Acta Radiol. 1993;34(4):356-61.

40. Andersen C, Taagehoj JF, Muhler A, Rehling M. Approximation of arterial input curve data in MRI estimation of cerebral blood-tumor-barrier leakage: Comparison between Gd- DTPA and Tc-99m-DTPA input curves. Magn. Reson. Imaging 1996;14(3):235-41.

41. Press WH, Teukolsky SA, Vetterling WT, Flannery BP. Numerical recipes in C. 2 ed. Cambridge, USA: Cambridge University Press; 1994.

42. Galea MH, Blamey RW, Elston CE, Ellis IO. The Nottingham Prognostic Index in primary breast cancer. Breast Cancer Res. Treat. 1992;22(3):207-19.

43. Furman-Haran E, Schechtman E, Kelcz F, Kirshenbaum K, Degani H. Magnetic resonance imaging reveals functional diversity of the vasculature in benign and malignant breast lesions. Cancer 2005;104(4):708-18.

44. Knopp MV, von Tengg-Kobligk H, Choyke PL. Functional magnetic resonance imaging in oncology for diagnosis and therapy monitoring. Mol. Cancer Ther. 2003;2(4):419-26.

45. Padhani AR. Dynamic contrast-enhanced MRI in clinical oncology: Current status and future directions. J. Magn. Reson. Imaging 2002;16(4):407-22.

46. Manton DJ, Chaturvedi A, Hubbard A, Lind MJ, Lowry M, Maraveyas A*, et al.* Neoadjuvant chemotherapy in breast cancer: early response prediction with quantitative MR imaging and spectroscopy. Br. J. Cancer 2006;94(3):427-35.

47. Padhani AR, Hayes C, Assersohn L, Powles T, Makris A, Suckling J*, et al.* Prediction of clinicopathologic response of breast cancer to primary chemotherapy at contrast-enhanced MR imaging: Initial clinical results. Radiology 2006;239(2):361-74.

Table 1

Table 1: Summary of histological status of breast cancer lesions

	Node positive	Node negative	Total
Grade 1	10	2	12
Grade 2	11	18	29
Grade 3	9	9	18
Total	30	29	59

Table 2

Table 2. Pharmacokinetic and "black-box" measured in two different lesions (with DCE-MRI curves presented in Figure 4.)

	ROI1 (Grade 1 node negative)	ROI2 (Grade 3 node positive)
ME	1.68	2.39
WOS [min^{-1}]	0.020	-0.008
IRE [min^{-1}]	0.690	1.833
v_e	0.275	0.535
K^{trans} [min^{-1}]	0.194	0.815
k_{ep} [min^{-1}]	0.706	1.523

Table 3

Table 3. Summary of black-box variables

	ME	IRE [min^{-1}]	WOS [min^{-1}]
Grade 1 (n =12)	2.04 (0.33)	1.32 (0.44)	0.017 (0.066)
Grade 2 (n =29)	2.20 (0.36)	1.50 (0.6)	-0.007 (0.056)
Grade 3 (n =18)	2.26 (0.29)	1.75 (0.48)	-0.035 (0.056)

Table 4

Table 4. Summary of pharmacokinetic variables

	v_e	K^{trans} [min^{-1}]	k_{ep} [min^{-1}]
Grade 1 (n =12)	0.39 (0.13)	0.61 (0.28)	1.62 (0.82)
Grade 2 (n =29)	0.46 (0.14)	0.91 (0.73)	2.04 (1.60)
Grade 3 (n =18)	0.46 (0.11)	1.41 (0.69)	3.17 (1.62)

Table 5

Table 5. Significance of the difference of pharmacokinetic variables K^{trans} and k_{ep} between tumour grades

	Grade 1 vs Grade 2	Grade 1 vs Grade 3	Grade 2 vs Grade 3
K^{trans}	n.s.	$p<0.005$	$p<0.05$
k_{ep}	n.s.	$p<0.01$	$p<0.05$

Table 6

Table 6: Correlations between DCE-MRI parameters and tumour grade (all correlation coefficients are Pearson's ρ, apart from those related to tumour grade, where Spearman's ρ is listed instead).

	ME	IRE	WOS	v_e	K^{trans}	k_{ep}
Tumour grade	0.228	0.274*	-0.334**	0.182	0.473**	0.420**
ME	1	0.817**	-0.013	0.981**	0.377**	0.027
IRE		1	-0.289*	0.747**	0.550**	0.299*
WOS			1	0.117	-0.563**	-0.626**
v_e				1	0.263*	-0.095
K^{trans}					1	0.910**
k_{ep}						1

* $p<0.05$

** $p<0.01$

Figures

Figure 1: Pre-contrast, post-contrast and subtraction image derived form a DCE-MRI dataset

Figure 2: Parametric maps of the variables ME (left), IRE (middle) and WOS (right) corresponding to the images presented in Figure 1

Figure 3: The ROI illustrated is superimposed onto a colour map of variable IRE. However, ROI selection was based on simultaneous inspection of all three parametric maps in Figure 2

Figure 4: Examples of dynamic curves from 2 ROIs derived form a Grade 1 lesion (left) and a Grade 3 lesion (right). DCE-MRI parameters are listed in Table 2

Figure 5. K^{trans} values for all tumours in the three histological groups

Figure 1

Click here to download high resolution image

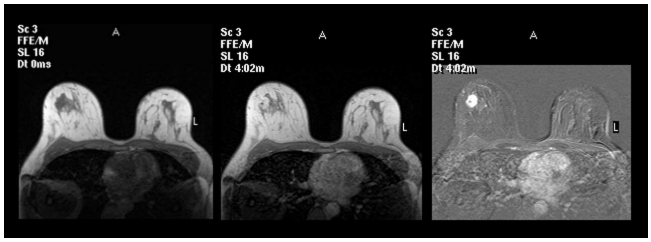

Figure 2

Click here to download high resolution image

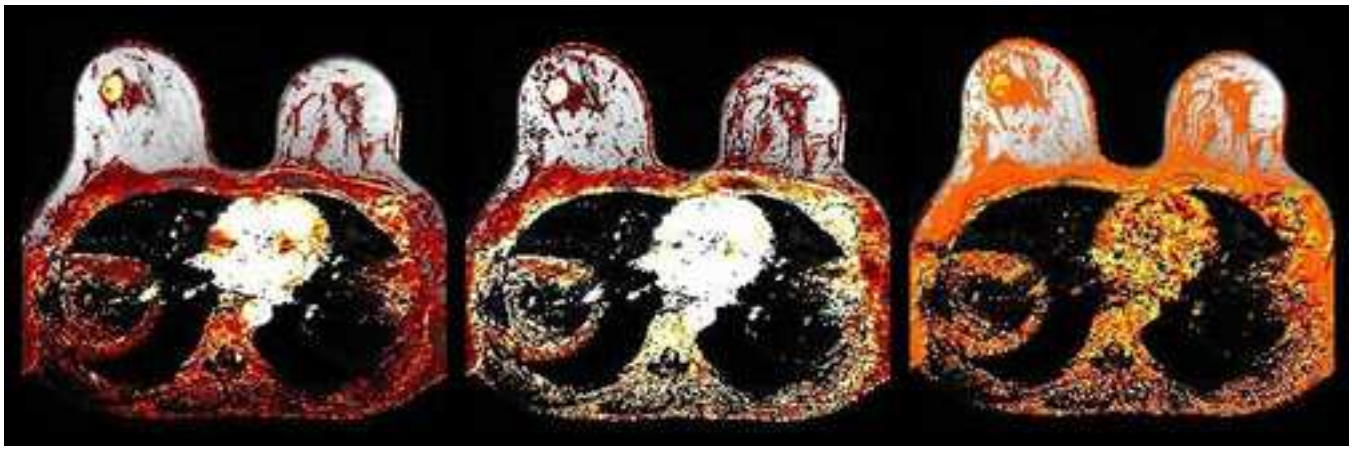

Figure 3

Click here to download high resolution image

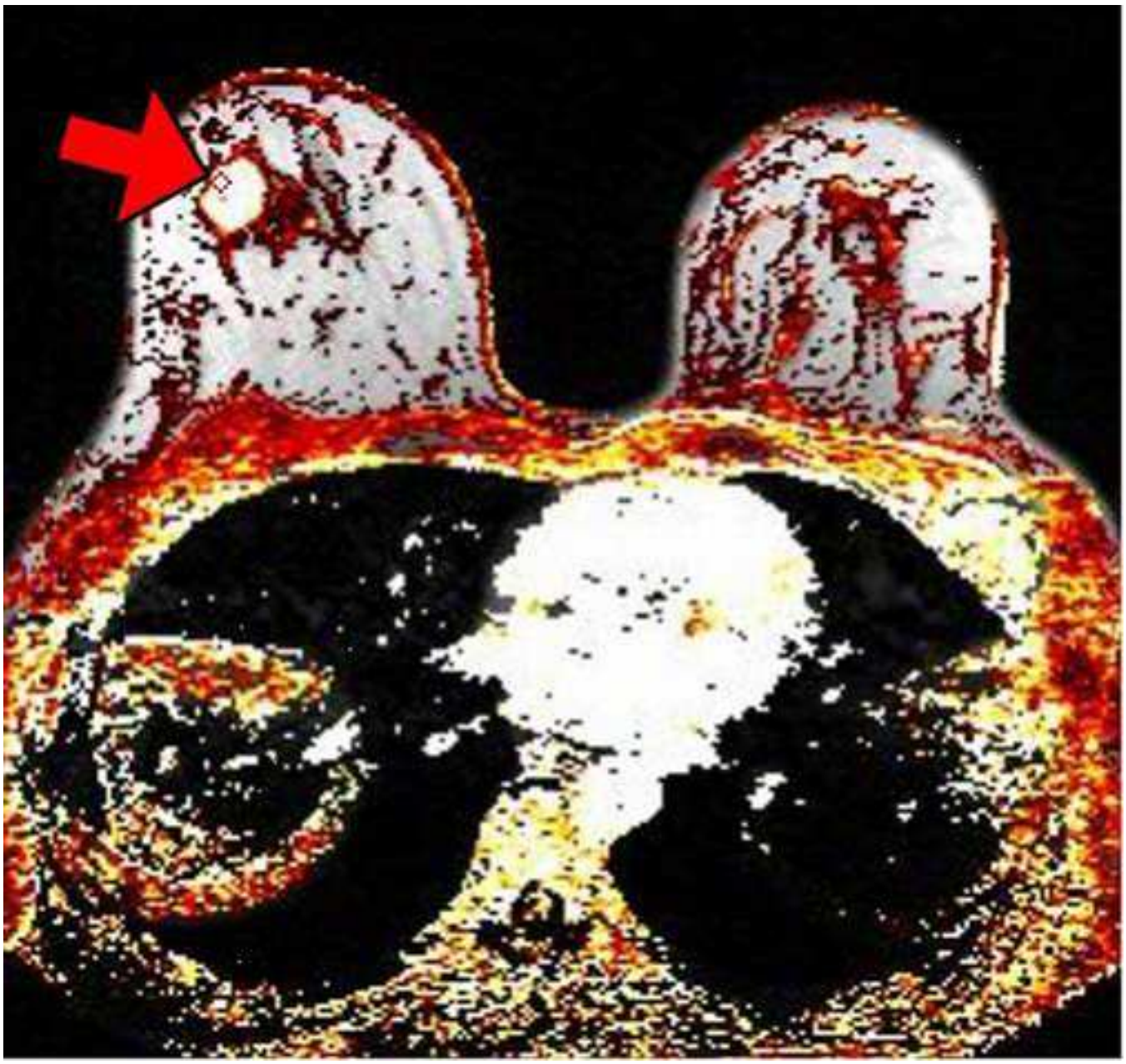

Figure 4

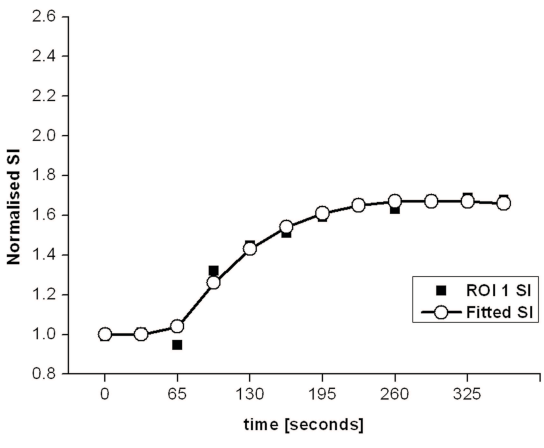
Normalised SI
2.6
2.4
2.2
2.0
1.8
1.6
1.4
1.2
1.0
0.8
0
65
130
195
260
325
time [seconds]
ROI 1 SI
Fitted SI

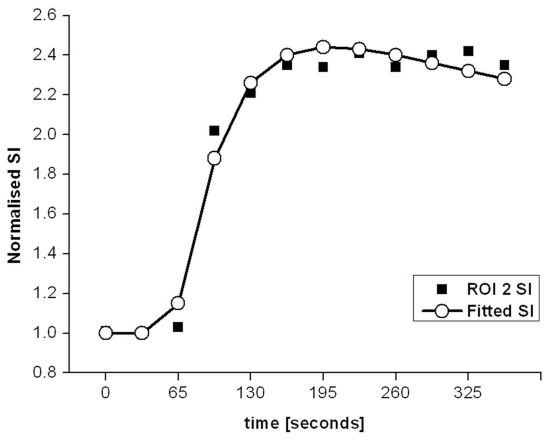
Normalised SI
2.6
2.4
2.2
2.0
1.8
1.6
1.4
1.2
1.0
0.8
0
65
130
195
260
325
time [seconds]
ROI 2 SI
Fitted SI

Figure 5